forests

MDPI

Article

Variability in the Hydrological Processes of Six Typical Woodlands Based on Stable Isotopes in Subtropical Regions in Central China

Fangfang Zhu [1,2], Yuchen Li [1,2] and Jinhua Cheng [1,2,*]

[1] College of Soil and Water Conservation, Beijing Forestry University, Beijing 100083, China; zhufangf@bjfu.edu.cn (F.Z.)
[2] Key Laboratory of Soil and Water Conservation and Desertification Control of State Forestry Administration, Beijing 100083, China
* Correspondence: jinhua_cheng@126.com

Abstract: Changes in woodland characteristics induced by plants and soil greatly affect soil hydrological processes. Stable isotope technology and indoor soil moisture characteristic experiments were conducted at three rainfall levels (3.6, 23.5, and 49.8 mm) to investigate the hydrological processes under six woodlands (two pure forests and four mixed forests). The main influencing factors contributing to these changes were identified in a low mountain and hilly region in central China. The soil waterline equation in this area was soil water $\delta D = 5.626\,\delta^{18}O - 16.791$ ($R^2 = 0.798$). The slope and intercept in the soil waterline equation were smaller than the atmospheric waterline equation. From a temporal perspective, the soil moisture content varied in the same trend under different rainfall events, with the maximum and minimum values on the first day after rainfall and the day before rainfall, respectively. However, an overall trend that first increased and then decreased was observed. From a spatial perspective, the soil moisture content increased with soil depth, and the increase rate was in the order of 0–20 cm and 20–40 cm in different soil layers. The soil moisture content in mixed conifer broadleaved woodlands was high. The soil water δD and $\delta^{18}O$ in mixed conifer broadleaved woodlands and underground soil were relatively depleted. The effects of soil water-holding capacity, particle size composition, slope, canopy closure, and other factors on soil hydraulic parameters were comprehensively analyzed. The results showed that the extremely coarse sand (1–2 mm) particle content was the main parameter affecting soil-saturated hydraulic conductivity K_s, whereas the slope was the main factor affecting soil water δD and $\delta^{18}O$. In needle-leaved forests, the soil water infiltration form was a rainwater and soil water mixture downward diffusion, whereas the rainwater replaced the original soil water in the needle and mixed conifer broadleaved forests.

Keywords: forests; soil hydrological property; soil waterline equation; stable isotopic composition

check for updates

Citation: Zhu, F.; Li, Y.; Cheng, J. Variability in the Hydrological Processes of Six Typical Woodlands Based on Stable Isotopes in Subtropical Regions in Central China. *Forests* **2023**, *14*, 1296. https://doi.org/10.3390/f14071296

Academic Editor: Mukesh Gautam

Received: 25 March 2023
Revised: 13 June 2023
Accepted: 20 June 2023
Published: 23 June 2023

Copyright: © 2023 by the authors. Licensee MDPI, Basel, Switzerland. This article is an open access article distributed under the terms and conditions of the Creative Commons Attribution (CC BY) license (https://creativecommons.org/licenses/by/4.0/).

1. Introduction

The water-holding function of the forest is influenced by water retention in the forest canopy [1], water absorption in the tree trunk [2], water storage in the litter layer [3], and water holding in the soil layer [4]. As a natural synthesis, the soil is composed of water, soil, and vegetation. In principle, soil moisture is an important factor in the interconnection between matter and energy in the soil–plant–atmosphere system; it is also a key factor controlling the ecosystem's structure [5–7]. Soil moisture exists in the unsaturated zone between the soil surface and the groundwater surface [8]. Vegetation also participates in the soil water cycle. Plant roots and leaves can absorb soil water and dissipate it into the atmosphere through transpiration consumption. Soil moisture affects vegetation growth and soil formation processes; it influences soil physical properties, such as soil structure and porosity [9]. Moreover, soil moisture can even affect the dissolution of trace elements and other biochemical reactions [10].

Soil moisture shows spatial variability under the influence of topography [11,12], vegetation [13], meteorology [14], land use type [15], and human activities [16]. Rainfall replenishment of soil water can barely exceed the depth of the 1 m soil layer in the Loess Plateau region [9]. Mei et al. [17] found that vegetation type plays a vital role in the impact of soil water change under non-drought conditions. The water-holding function varies greatly because of the differences in morphological characteristics and community structure of tree species [18,19]. Remarkable differences can be found in canopy interception, evaporation of stands, and root uptake capacity of different tree species [20,21]. Therefore, the vegetation type [9] and growth condition are factors that cannot be ignored in studying soil water characteristics in woodlands [22,23].

As a key limiting factor for forest survival [24], the study of soil water in different stands has received attention from many scholars [25]. At present, most studies focus on seasonally dry areas and perennially dry areas, such as the Loess Plateau [26,27]. Ilek et al. [28] compared the dynamic changes in the soil moisture in *Fagus sylvatica* L. and *Abies alba* Mill. They found significant differences between them during dry periods. Moreover, forest stand density can influence rainwater infiltration. The response ability of rainfall to deep soil improves when the density stand is low, and the canopy structure is reasonable [29]. Tian et al. [30] studied the effects of different vegetation covers on the soil moisture response. They found that the soil water increase rate decreases with soil depth. Deep-rooted soils have a higher water transport capacity than the soil where the shallow roots are located. Fang et al. [31] analyzed the deep soil moisture change in the 80–500 cm soil layer in the Loess Plateau. They concluded from their analysis that lemongrass and acacia caused a severe drought. The soil water deficits in different woodlands have significant differences. Nevertheless, the highest soil moisture content was found in the false acacia red pine stand, and the lowest was found in the Simone red pine stand [32]. Wei et al. [21] compared the characteristics of hydraulic redistribution in different forests. They found that hydraulic redistribution was frequently triggered within a depth of 30 cm in evergreen mixed conifer broadleaved forests.

Stable hydrogen and oxygen isotope technology is used to obtain effective soil moisture information on soil moisture movement patterns, infiltration, and recharge and is used to reveal information on hydrological processes in the soil [33]. The form of soil moisture infiltration can be judged by studying the distribution difference of isotopes in soil moisture in different soil layers [34]. Soil moisture dynamics change law is the basis for exploring the water balance of a woodland, which usually has temporal and spatial dimensions, namely temporal variation and vertical variation. The differences in the soil moisture distribution in the profile are the expression of soil moisture spatial heterogeneity, which depends mainly on the distribution characteristics of plant roots [35]. Deep-rooted plants, such as trees and shrubs, can utilize deep and shallow soil water. Furthermore, the growth statuses of the primary and lateral roots are related to the soil moisture's longitudinal and transverse movements, respectively [36].

In regions with the same climate, vegetation is the dominant factor in the spatiotemporal distribution of soil water. Several factors, such as canopy cover [37], atmospheric precipitation, and topsoil evaporation, can change the stable isotopes of hydrogen and oxygen in soil water [38]. Vegetation has different responses to rainfall types, and the water use regimes of plants change significantly before and after rainfall [39]. The deep soil below 40 cm is less susceptible to evaporation and rainfall effects than the topsoil; moreover, the isotopic value of the former was more stable than the latter [40].

The low mountain and hilly regions in central China have an overall humid climate and high rainfall. However, the rainfall event distributions are uneven in time and space. Thus, determining the characteristics of temporal and spatial variabilities of woodland soil moisture and its limiting factors in this area is crucial. Rainfall conditions and woodland characteristics have a significant impact on hydrological processes. Few studies systematically consider the regulatory mechanism of soil physical properties, forest vegetation structure, and rainfall on the upper soil hydrological process. In the present study, the

method combining indoor soil moisture characteristic experiments and natural rainfall experiments aims to study the soil hydrological properties and their influences on typical woodlands in the Taizishan area. Moreover, the hydrogen and oxygen stable isotope technology provides information on soil moisture movement. This study describes the soil hydrological processes from temporal and spatial dimensions, thereby revealing the regulatory mechanism of protective forests on hydrological processes and their response to changes in precipitation patterns.

2. Materials and Methods

2.1. Research Area

The Taizishan Forest in Hubei Province is located in the north–south transition zone of China, with coordinates of 112°48′45″–113°03′45″ E, 30°48′30″–31°02′30″ N (Figure 1). The research area is in a subtropical monsoonal humid climate area. It is rainy in summer and autumn and dry in winter and spring. Rainfall is concentrated in summer, with an average annual rainfall of 1094.6 mm. The interannual variation in precipitation is significant, with minimum and maximum values of 862 and 1708 mm, respectively. The annual average temperature is 16.4 °C. The area has obvious karst topography, and the terrain gradually decreases from the northeast to the southwest, with an altitude of 40.3–467.4 m. The soil is a clayey yellow-brown soil layer developed from loess parent material with a thickness of approximately 0.7–1.5 m and is slightly acidic. The composition of soil particles is shown in Table 1. The canopy cover of this forest, including natural vegetation, artificial vegetation, and herbs, can reach 80%. The natural vegetation is dominated by *Quercus acutissima Carruth.*, and the artificial vegetation is dominated by coniferous species, such as *Pinus massoniana (Lamb.)*, *Cupressus funebris Endl.*, and *Cunninghamia lanceolata (Lamb.) Hook*. The herbs are dominated by simple plants, such as fern and *Miscanthus floridulus (Labill.) Warb*.

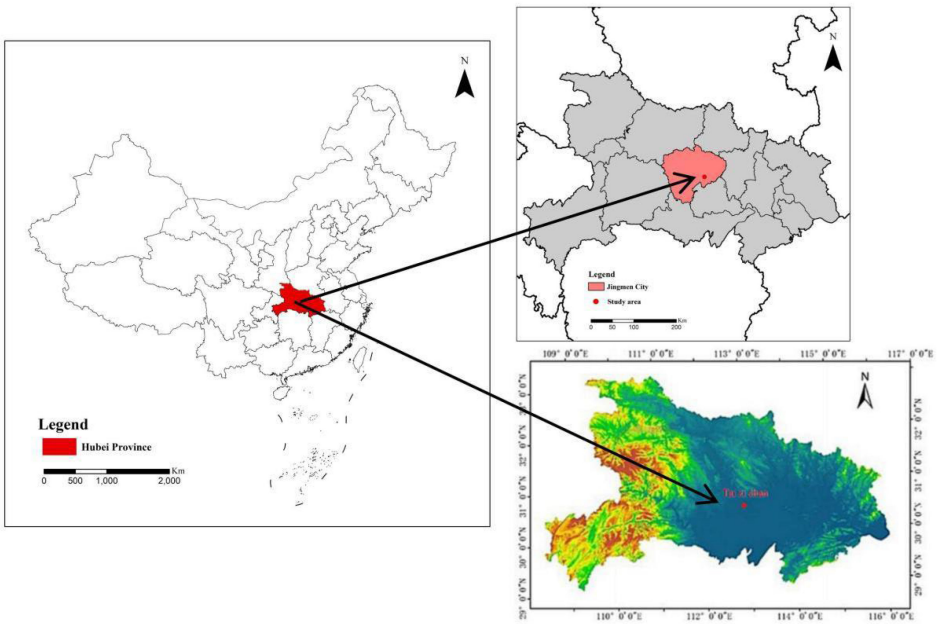

Figure 1. The geographic location of the study area.

Table 1. Soil particle composition of the six woodlands.

Woodlands	Clay	Fine Silt	Coarse Silt	Fine Sand	Medium Sand	Coarse	Very Coarse Sand
	≤0.002 mm	0.002–0.02 mm	0.02–0.05 mm	0.05–0.25 mm	0.25–0.5 mm	0.5–1 mm	1–2 mm
P. massoniana Lamb. (PML)	40.65	47.61	2.89	3.31	1.3	4.24	0
C. funebris Endl. (Cf)	31.79	52.75	10.19	1.9	0.89	2.48	0
C. funebris Endl. and Ilex chinensis Sims. (Cl)	22.36	53.16	21.77	2.71	0	0	0
P. massoniana Lamb. and C. funebris Endl. (PC)	21.09	52.71	23.21	2.99	0	0	0
P. massoniana Lamb. and I. chinensis Sims. (Pl)	29.87	56.19	11.93	1.87	0.14	0	0
P. massoniana Lamb. and Cinnamomum camphora (Linn.) Presl. (PCin)	25.08	56.71	15.67	2.54	0	0	0

2.2. Observation of Meteorological Factors

A Vantage Pro2 Type Automatic Weather Station was installed in the open area near the experimental plots to monitor the temperature, rainfall, rainfall intensity, air humidity, wind speed, and other meteorological factors in real-time. In this study, it was mainly used to record the time of rainfall and ensure that no rainfall event occurred before the experiment. The temperature and precipitation during sampling periods are shown in Figure 2.

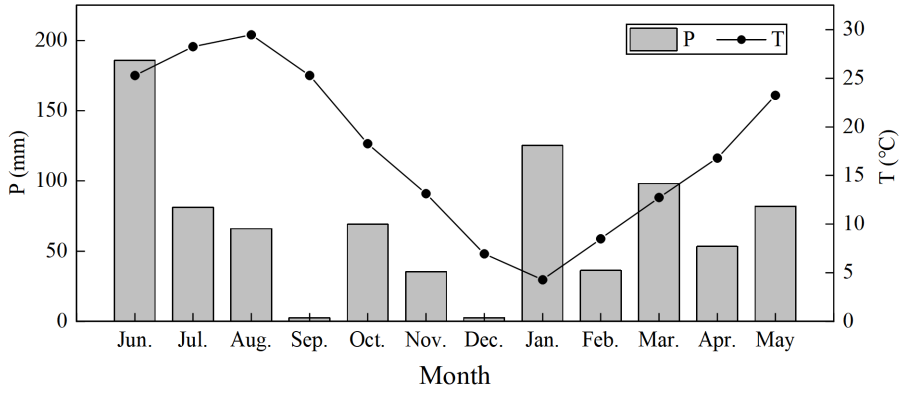

Figure 2. Temperature and precipitation during sampling periods.

2.3. Soil Sample Collection and Storage

Three soil profiles with a depth of 40 cm were dug within a radius of 1 m at the center of each standard plant at each site. Each 10 cm of soil is divided into one layer and marked as S0, S1, S2, and S3. S0 is the 0–10 cm soil layer; S1 is the 10–20 cm soil layer; S2 is the 20–30 cm soil layer; and S3 is the 30–40 cm soil layer. Three samples were taken as replicates in each site according to the upper, middle, and lower slopes. In the sampling session, the soil samples were taken with a TST-55 ring cutter, a penetrometer, a 100 cm^3 ring knife, and a soil auger. Three replicate samples were collected from each soil layer. The soil samples were used to determine the soil-saturated hydraulic conductivity, water penetration curves, soil moisture content, hydrogen and oxygen isotope content in soil water, and other soil physical properties.

During the observation period, the samples (soil and rainwater) with rainfall greater than 1 mm were collected each time (Figure 3). The sampling period is 1 day before and 3 days after rainfall. This study conducted eight sampling sessions. Based on the amount of

rainfall, three rainfall events of 3.6 mm (light rain), 23.5 mm (moderate rain), and 49.8 mm (heavy rain) were selected as the research objects. The soil sample storage requirements were relatively high because of the determined hydrogen and oxygen isotope content. However, the soil sample collection process should focus on sealing and freezing. After being sealed with Parafilm, the sample bottles were quickly placed in an insulated cabinet at a temperature of 0–5 °C (in the field) and then kept in a freezer at a temperature of −5 °C for a long time. The sampling time chosen was a day with no rainfall events occurring 3 days before to keep the soil moisture stable [41].

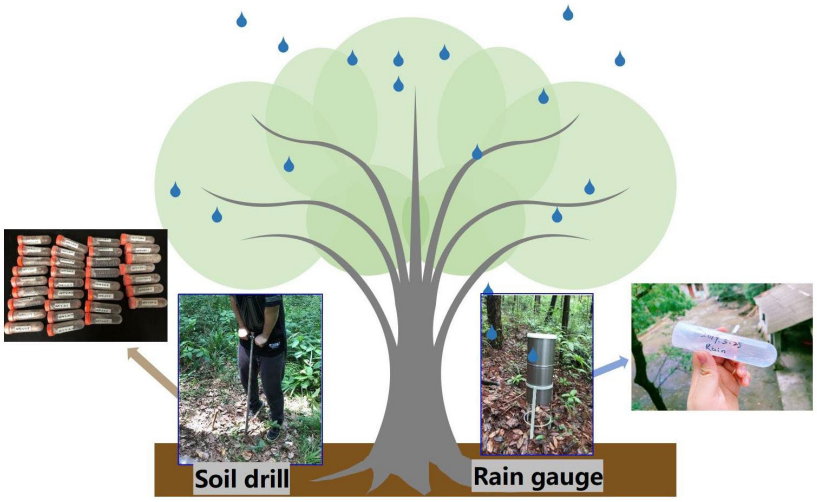

Figure 3. Sample collection diagram.

2.4. Stable Isotopes of Hydrogen and Oxygen

The water from the soil samples was extracted with an LI-2100 automated vacuum distillation system (LI-2100, LICA, Beijing, China). An isotope ratio mass spectrometer (Finnigan Delta V Advantage, Thermo Fisher Scientific, Inc., Waltham, MA, USA) and an elemental analyzer (Flash 2000HT, Thermo Fisher Scientific, Inc., Waltham, MA, USA) were used to determine the extracted water samples and analyze the stable isotope composition of hydrogen and oxygen in each sample.

Isotopic ratios were expressed in thousands of differences from the Vienna Standard Mean Ocean Water (V-SMOW). Its formula is as follows:

$$\delta‰ = \left(R_{sample}/R_{standard}\right) \times 1000, \quad (1)$$

where R_{sample} and $R_{standard}$ represent the molar abundance ratios of the sample and V-SMOW (D/H, $^{18}O/^{16}O$), respectively. The measurement precision was consistently ±2‰ for δD and ±0.2‰ for $\delta^{18}O$.

2.5. Soil-Saturated Hydraulic Conductivity

In this study, the soil-saturated hydraulic conductivity was determined using the Mariotte bottle steady head method [42]. The water surface height in the Mariotte bottle was always maintained at 10 cm. The infiltration water amount was measured every 10 min for 30 s during the 1st hour of the test. Subsequently, the infiltration was measured every 30 min for 30 s.

Soil-saturated hydraulic conductivity K_s is the amount of water passing through a unit area under a unit water potential gradient and unit time when the soil is saturated with water. It was computed as:

$$K_s = \frac{V}{tA} \cdot \frac{L}{H}, \quad (2)$$

where K_s is the saturation hydraulic conductivity in cm·min^{-1}. H is the water surface height at the inlet end in cm. V is the water outflow rate in mL. L is the length of the soil column in cm. t is the water outflow time in min. A is the cross-sectional area of the soil column in cm^2.

2.6. Soil Water Characteristic Curves

Before the test started, the soil samples were soaked in 20 °C water for 12 h. Then, they were padded with filter paper and placed in a dry and ventilated place for 12 h to make the soil moisture content reach the field water-holding capacity. The temperature of the environment where the samples were kept after soaking was 25 °C. Subsequently, the soil sample was placed in the TST-55 soil water permeameter, and the water surface height of the Mariotte bottle was kept at 8 cm. When the water flowed out, the water samples were collected every 5 s until the flow reached stability. In this study, the soil infiltration rate was determined by the Mariotte bottle steady head method. The temperature was the main influencing factor of the soil infiltration function. Thus, soil infiltration rates were uniformly converted to infiltration rates at 10 °C.

Their calculation formulas are as follows:

$$K_t = \frac{10 \times Q_n \times L}{t_n \times A \times (H + L)}, \quad (3)$$

$$K_{10} = \frac{K_t}{0.7 + 0.03 \times t}, \quad (4)$$

where K_t is the soil infiltration rate in mm·min^{-1}. K_{10} is the infiltration rate at 10 °C, with the unit of mm·min^{-1}. Q_n is the amount of water collected in 5 s, with the unit of ml. t is the infiltration interval in min.

2.7. Soil Dynamic Moisture Monitoring

The Watchdog 1400 soil moisture and temperature monitoring station was used to measure soil moisture and temperature. The measured soil depth was 40 cm. Four instrument probes were used, and one was placed in every 10 cm soil layer. The monitoring period was from June to August 2021, and the frequency was once a minute.

3. Results

3.1. Basic Physical Properties of Soil

3.1.1. Soil Porosity Characteristics

Soil porosity is a vital indicator of soil compactness and is positively correlated with water transport and soil storage. This study mainly explores the relationship between microporosity and soil hydrological effects. In this experiment, the variation ranges of soil total porosity (TP), capillary porosity (CP), and noncapillary porosity (NY) were 42.4%−64.9%, 27.8%−39.8%, and 14.1%−26.4%, respectively (Figure 4). Compared with the various degrees of TP, CP, and NY in different woodlands, those in PCin were the highest, with a variation coefficient ranging from 0.075 to 0.189. The variation coefficients with TP, CP, and NY in PCin were 15.779%, 13.821%, and 20.915% higher than other woodlands.

Cf has the lowest degree of variation, with variation coefficients ranging from 0.086 to 0.369. The percentage of CP was 50% more than NY within each woodland, and CP was consistent with the changing pattern of TP. TP was taken as the key index of soil pore characteristics. As a result, the TP in the 30−40 cm soil layer was 15.515% smaller than the 0−10 cm soil layer. Furthermore, the TP of Cf decreased with the soil depth. Moreover, the TP of other woodlands initially experienced troughs and peaks successively, which fluctuated in the inverted 'N' shape but showed a downward trend overall.

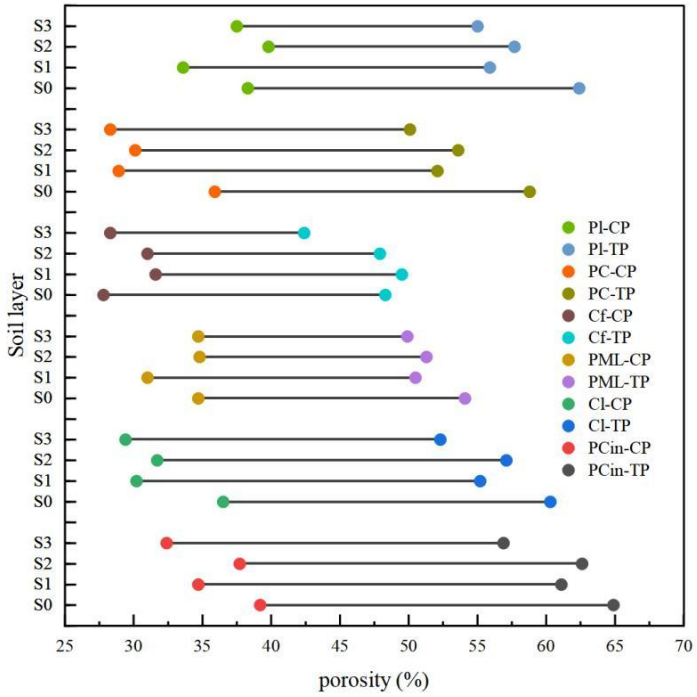

Figure 4. Soil porosity characteristics of the six woodlands.

3.1.2. Soil Water-Holding Capacity

The maximum values of soil maximum water−holding capacity (MAC), minimum water-holding capacity (MIC), and field water-holding capacity (FWC) were all found in the 0−20 cm soil layer (Figure 5). The variation ranges of MAC, MIC, FWC, and natural moisture content were 0.459−0.765, 0.274−0.426, 0.236−0.409, and 0.175−0.297, respectively. From the perspective of soil depth, the overall trend decreased with increasing soil depth. The MIC of soil was inconsistent with the MAC and FWC with soil depth, and a highly significant positive correlation existed between them ($p < 0.01$).

The MIC was selected as the soil water-holding performance index through the principal component analysis method. The order of the soil water-holding capacity of the six woodlands was PCin, Pl, Cl, PC, Cf, and PML. Three significant relationships were obtained by comprehensively analyzing the correlation between the seven indexes of soil water-holding capacity. A very significant positive correlation existed between MIC and soil porosity ($p < 0.01$), MAC and TP had a significant positive correlation ($p \leq 0.05$), and TP had a significant positive correlation with MIC, MAC, and FWC ($p \leq 0.05$).

3.2. Soil Hydrological Characteristics

3.2.1. Soil-Saturated Hydraulic Conductivity

The soil-saturated hydraulic conductivity varied greatly between woodlands (Figure 6). The variation ranges of the soil-saturated hydraulic conductivity in the six woodlands were 1.256−5.670 (PCin), 1.190−2.857 (Cl), 0.678−1.256 (PML), 0.406−0.856 (Cf), 0.912−1.923 (PC), and 1.245−4.614 (Pl). Overall, the soil-saturated hydraulic conductivity of different woodlands was significantly different. The soil−saturated hydraulic conductivity of the PCin woodland was the largest, and the variation coefficient was 1.635. However, the soil-saturated hydraulic conductivity of the Cf woodland was the smallest, and the variation coefficient was 0.679. The comprehensive analysis of the soil-saturated hydraulic conductivity variation law in the six woodlands indicated that the order was PCin, Pl, Cl, PC, PML, and Cf. In the soil profile, the soil-saturated hydraulic conductivity varied with the soil depth decrease first, then increased, and finally decreased. The maximum and minimum numerical values of soil-saturated hydraulic conductivity were in the 0−10 cm

and 30−40 cm soil layers, respectively. Furthermore, the saturated hydraulic conductivity of the topsoil was 60.073% higher than the deep soil.

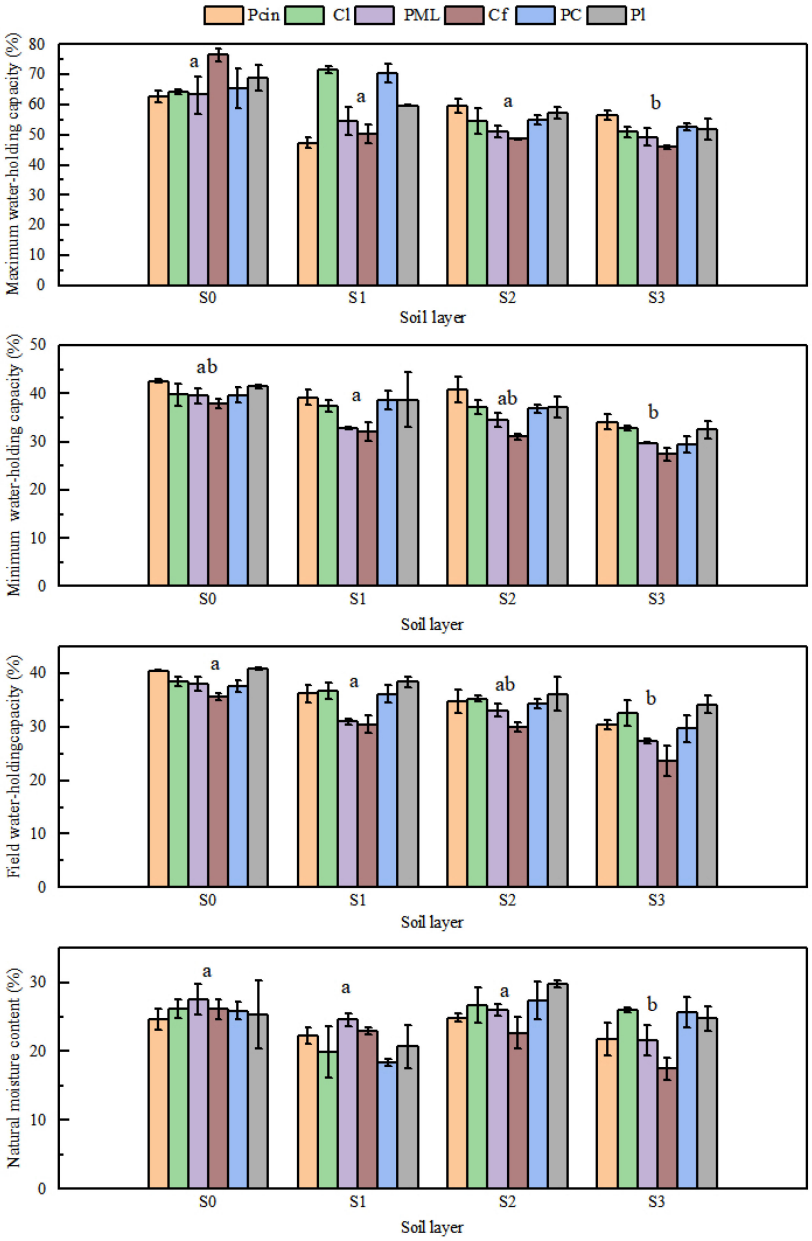

Figure 5. The water-holding capacity of different soil layers in the six woodlands. The vertical lines in the figure are error bars. Different letters indicate significant differences between different filter materials at the 0.05 level.

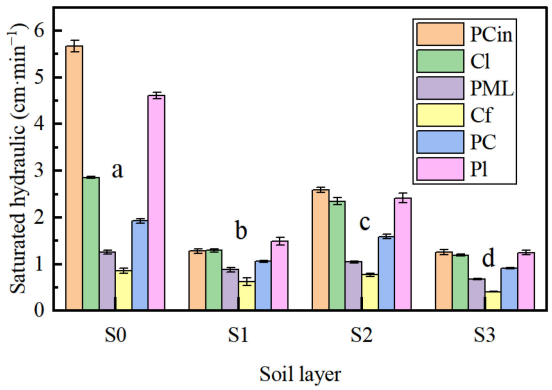

Figure 6. Soil−saturated hydraulic conductivity of the six woodlands. The vertical lines in the figure are error bars. Different letters indicate significant differences between different filter materials at the 0.05 level.

3.2.2. Soil Moisture Characteristic Curves

The soil moisture characteristic curves of different woodlands have a significant difference (Figure 7). The outlet rate rapidly increased first with the test time and then stabilized. Fluctuations in the soil water penetration curve mainly occurred in the first 60 s. The volatility of the soil water penetration curve was significantly high in the PCin, Pl, and Cl woodlands. Compared with the outlet rates of other soil layers, the outlet rate of the 30−40 cm soil layer was the first to reach a steady state. The variation ranges in the outlet rates of PCin, Pl, Cl, PC, PML, and Cf were 0.98−1.80, 0.68−1.54, 0.52−1.68, 0.46−1.16, 0.46−0.76, and 0.34−0.98, respectively. The variation range of Pl was the largest, and PML was the smallest. The comparison of the average soil outflow rates of the six woodlands indicated that the order of average soil outflow rates was PCin, Pl, Cl, PC, PML, and Cf. PCin had the highest average soil outflow rates, and it was followed by Pl, Cl, PC, PML, and Cf.

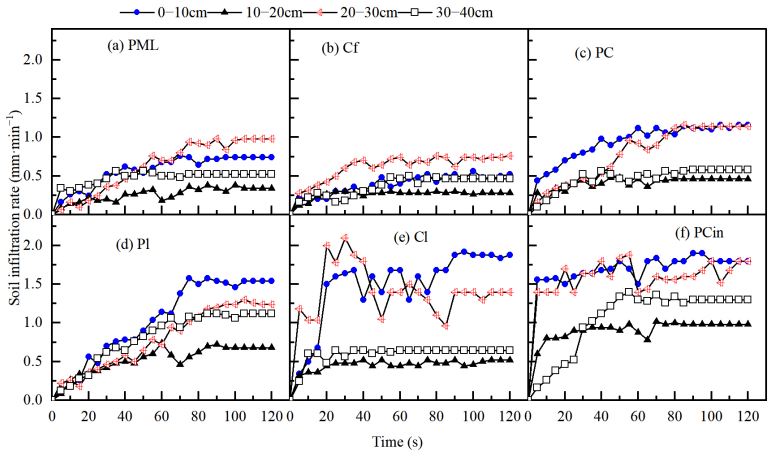

Figure 7. Soil moisture characteristic curves of the six woodlands. Cf is *C. funebris Endl.* woodland; PC is *P. massoniana Lamb.* and *C. funebris Endl.* mixed woodland; Pl is *P. massoniana Lamb.* and *I. chinensis Sims.* mixed woodland; Cl is *C. funebris Endl.* and *I. chinensis Sims.* mixed woodland; PCin is *P. massoniana Lamb.* and *Cinnamomum camphora (Linn.) Presl.* mixed woodland.

3.2.3. Soil Infiltration Rate

The soil infiltration characteristics of the six woodlands are shown in Figure 8. The variation ranges of soil initial and stable infiltration rates were 2.759−38.963 and 1.736−24.263, respectively. The soil initial infiltration rate varied in the range of 0.619−1.72, with PC and Cf exhibiting the largest and smallest values, respectively (Figure 8a). The soil stable

infiltration rate varied in the range of 0.559−1.635, with PCin and PML exhibiting the largest and smallest values, respectively (Figure 8b). Overall, the initial infiltration rate of soil was higher than the stable infiltration rate. However, the soil initial and stable infiltration rates in Cf were smaller than the other woodlands. The comparison of the six woodlands indicated that the order of average soil infiltration rates was PCin, Pl, Cl, PC, PML, and Cf.

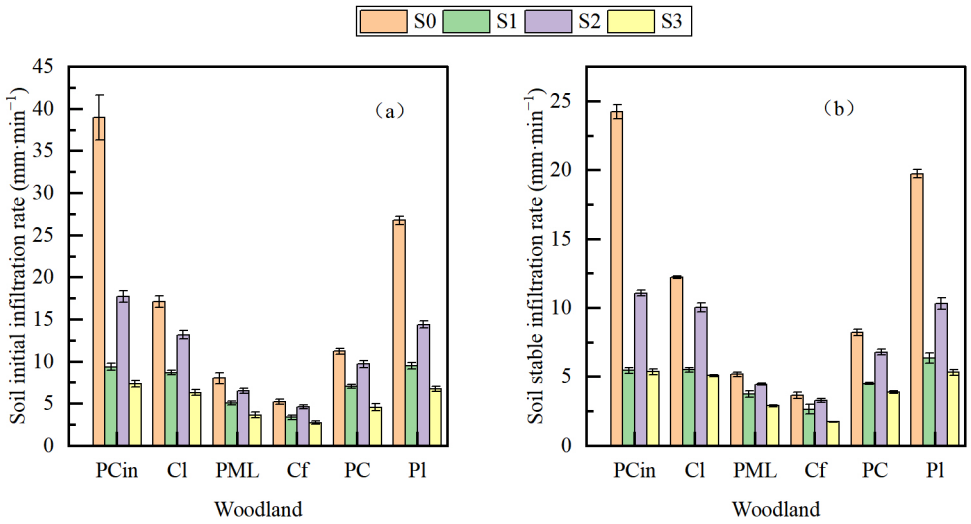

Figure 8. Soil infiltration rate of the six woodlands. PML is *P. massoniana Lamb.* woodland; (**a**) is the soil initial infiltration rates; (**b**) is the soil stable infiltration rates; Cf is *C. funebris Endl.* woodland; PC is *P. massoniana Lamb.* and *C. funebris Endl.* mixed woodland; Pl is *P. massoniana Lamb.* and *I. chinensis Sims*. mixed woodland; Cl is *C. funebris Endl.* and *I. chinensis Sims.* mixed woodland; PCin is *P. massoniana Lamb.* and *Cinnamomum camphora (Linn.) Presl.* mixed woodland. S0 is the 0−10 cm soil layer; S1 is the 10−20 cm soil layer; S2 is the 20−30 cm soil layer; S3 is the 30−40 cm soil layer.

The soil initial and stable infiltration rates showed fluctuations with soil depth, which first decreased rapidly, then increased slowly, and finally slowed down. The overall change was the 'W' type. The infiltration rate of the 0−10 cm soil layer was the highest, whereas the 10−20 cm soil layer was the lowest. Compared with the soil infiltration rate between each soil layer, the infiltration rate between the 0−10 cm soil layer and the 10−20 cm soil layer varied.

3.3. Soil Moisture Content

Soil moisture is in a dynamic change state without stable regularity, and it possesses temporal and spatial variations. These two characteristics are diurnal and vertical variations in soil moisture content. Furthermore, the order of soil moisture content in the six woodlands was PCin, Pl, Cl, PC, PML, and Cf (Figure 9). The vertical spatial perspective indicated that soil moisture content increased with soil depth. The increased rate of soil moisture content in the 0−20 cm soil layer was higher than the 20−40 cm soil layer. The trends of soil moisture content changes on the time scale under different rainfall events were consistent. The soil moisture content varied as follows: the maximum was reached on the first day after the rainfall event, and the lowest was reached on the day before the rainfall event. In general, it increased first and then decreased.

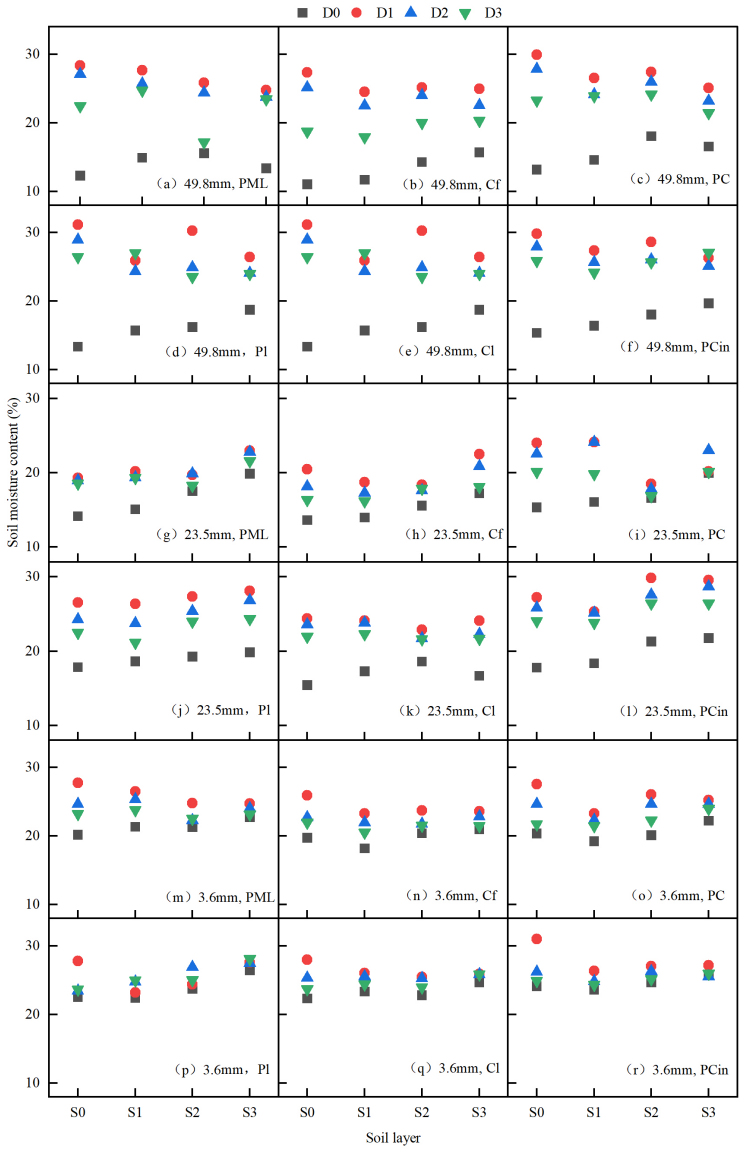

Figure 9. Changes in soil moisture content in the six woodlands under different rainfall events.

The occurrence of rainfall events can enhance the soil moisture content. Under 3.6 mm of rainfall, the soil moisture content increased by 17.34%, 10.95%, and 6.63% 3 days after the rainfall event. Under 23.5 mm of rainfall, the soil moisture content increased by 35.64%, 29.81%, and 20.70% 3 days after the rainfall event, respectively. Under 49.8 mm of rainfall, the soil moisture content increased by 81.32%, 66.97%, and 53.41% 3 days after the rainfall event. As shown above, the soil moisture content increase was the largest on the first day after the rainfall event, and it gradually decreased with time.

The comparison of the soil moisture content increases on the first day after rainfall in different soil layers indicated that the largest values were found in the 0−10 cm soil layer, whereas the smallest values were found in the 30−40 cm soil layer. The soil moisture content on the day before rainfall in different woodlands was thoroughly studied. The soil moisture content increased by 6.63%, 22.33%, and 51.94% after the rainfall events with 3.6 mm (light rain), 23.5 mm (medium rain), and 49.8 mm (heavy rain). Under the same rainfall events, the increased range of soil moisture content in different woodlands was significantly different. On the first day after rainfall, the growth rate of the soil moisture content decreased with increasing soil depth, and the second and third days after rainfall had no unity law.

At 3.6 mm of rainfall, the growth rate of the soil moisture content in PML and Pcin decreased with increasing soil depth. The growth rate of the soil moisture content in the 10–20 cm soil layer of Cf was the largest. Moreover, the maximum growth rates of soil moisture content in PC and Pl were in the 20−30 cm and 10−20 cm soil layers on the second and third days after rainfall, respectively. The maximum growth rate of soil moisture content in Cl was in the 20−30 cm and 0−10 cm soil layers on the second and third days after rainfall, respectively. Under 22.5 mm of rainfall, the growth rate of soil moisture content in other woodlands decreased with time and soil depth, except in PC. The growth rate of the soil moisture content in all woodlands decreased with time and soil depth at 49.8 mm of rainfall.

3.4. Hydrogen and Oxygen Isotope Characteristics in Soil Water

3.4.1. Soil Water δD Isotopic Change Characteristics

The response of soil water δD to different rainfall events is shown in Figure 10. When rainfall amounts were 3.6, 23.5 and 49.8 mm, the soil water δD content variation ranges were −58.48 to 25.89, −67.91 to 25.14, and −82.34 to 23.16, respectively. Therefore, the greater the amount of rainfall, the greater the soil water δD content variation range. Compared with the soil water δD average increment on the first day before rainfall, the soil water δD average increments when rainfall amounts were 3.6, 23.5, and 49.8 mm were 41.474%, 57.027%, and 89.365%, respectively. Thus, the increment of soil water δD increased with the increase in rainfall. In general, soil water δD decreased first and then increased with time. The maximum and minimum values of soil water δD appeared the day before rainfall and the first day after rainfall, respectively. The minimum value of soil water δD in the area occurred in PCin on the first day after 49.8 mm of rainfall.

Under 49.8 mm of rainfall (Figure 10a−f), the soil water δD of PML, Cf, and PC stands was much greater than the value of rainfall δD. At the same time, the soil water δD values of the 20−30cm soil layer in Pl and Cl were close to rainfall δD, which was closest to the rainfall δD value in the 10−20 cm soil layer of PCin. Under 23.5 mm of rainfall (Figure 9g−l), the soil water δD values of the 10−20 cm soil layer in PML, Cf, and PC were closest to the rainfall δD value, and the 0−10 cm soil layer in other woodlands were closest to the rainfall δD value.

Under 3.6 mm of rainfall (Figure 10m−r), the rainfall δD values were greater than the soil water δD values in Pl and PCin. The dispersion degree of soil water δD variation curves among soil layers varied under different rainfall amounts. The soil water δD variation curves of the four soil layers were the most and least discrete under 49.8 and 3.6 mm of rainfall, respectively.

The soil infiltration process of rainwater was inferred from the trend of soil water δD in each soil layer. Under 49.8 mm of rainfall, the value of rainwater δD was depleted compared with the value of soil water δD before rainfall. However, the soil water δD decreased and then increased with time after the rain in all soil layers except for the 30–40 cm soil layer. This finding indicated that soil water was slowly infiltrating. By contrast, the soil water δD before rainfall enriched the 30–40 cm soil layer on the third day after rainfall (Figure 10a,c). Moreover, the soil water δD values did not show significant fluctuations in the 30–40 cm soil layer. These results proved that the soil infiltration in PC did not reach the 30–40 cm soil depth. The rainwater δD values were within the range of soil water δD values and close to the soil water δD values before rainfall under 23.5 mm of rainfall. The soil water δD in the 10–20 cm soil layer was always the smallest among the other soil layers in all woodlands, except PML and Cl (Figure 10g–l). Compared with the soil water δD values before rainfall, the rainwater δD values were enriched in PCin and Cl under 3.6 mm of rainfall. The soil water δD values in the 30–40 cm soil layer in PML decreased with time after rainfall.

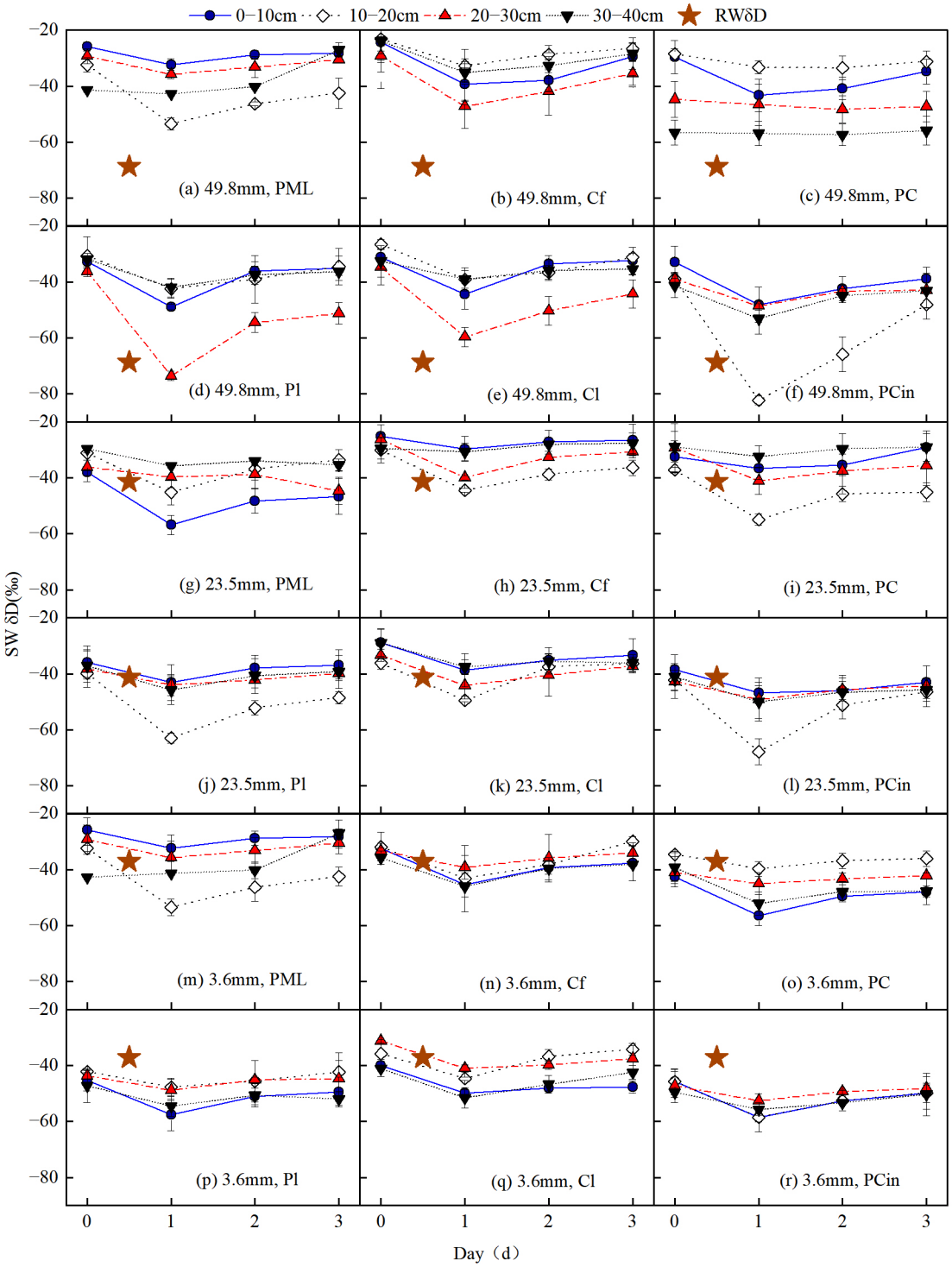

Figure 10. Changes in stable isotopic composition in the six forest lands under different rainfall events. RWδD. is rainfall δD. SWδD is soil water.

3.4.2. Soil Water $\delta^{18}O$ Isotopic Change Characteristics

The response of soil water $\delta^{18}O$ to different rainfall events is shown in Figure 11. The variation ranges of soil water $\delta^{18}O$ at 0−10 cm, 10−20 cm, 20−30 cm, and 30−40 cm soil layers were −6.430 to −1.762, −10.048 to −1.641, −11.035 to −1.712, and −6.574 to −1.302, respectively. Overall, the variation range of soil water $\delta^{18}O$ first increased and then decreased with soil depth. The mean values of soil water $\delta^{18}O$ at 0−10 cm, 10−20 cm,

20−30 cm, and 30−40 cm soil layers were −3.922, −4.370, −4.305, and −3.977, respectively. Thus, the mean values of soil water $\delta^{18}O$ decreased and then increased with soil depth.

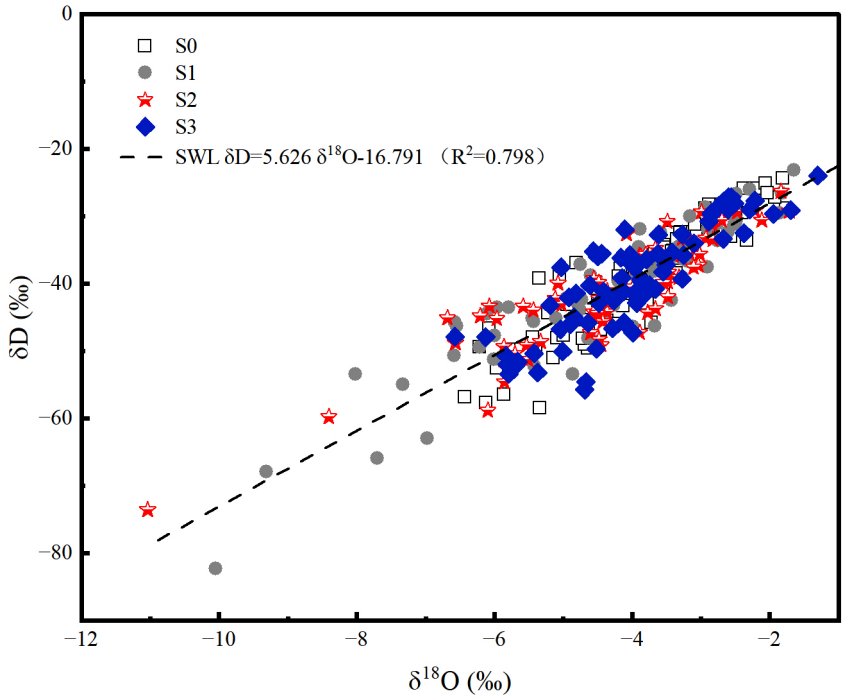

Figure 11. The relationship between hydrogen and oxygen isotopes in the soil water of the Taizishan Mountain area. S0 is the 0−10 cm soil layer; S1 is the 10−20 cm soil layer; S2 is the 20−30 cm soil layer; S3 is the 30−40 cm soil layer. SWL is the soil waterline equation.

3.4.3. The Functional Relationship between Soil Water δD and $\delta^{18}O$

The soil waterline equation was a linear relationship between soil water δD and $\delta^{18}O$. Furthermore, the slope indicated the fractionation ratio of soil water δD and $\delta^{18}O$, and the constant term (intercept) indicated the degree of deviation from the equilibrium state [43]. The relationships between soil water δD and oxygen $\delta^{18}O$ isotopes in the Taizishan area are shown in Figure 11. The slope and intercept in the soil waterline equation were smaller than the atmospheric waterline equation $\delta D = 8.01\delta^{18}O+10.28$ ($R^2 = 0.97$) [41].

The linear relationships of soil water δD and $\delta^{18}O$ in the six woodlands are shown in Figure 12. As shown above, significant differences were detected in soil water hydrogen and oxygen isotope contents under different woodlands in this study ($p < 0.05$). The results could be obtained through the linear fitting of soil water hydrogen and oxygen isotopes in the six woodlands (Figure 12). The slopes in the soil waterline equation were smaller than the atmospheric waterline equation in the Taizishan area. Nevertheless, PML had the maximum slope, followed by PCin, Cf, Cl, Pl, and PC.

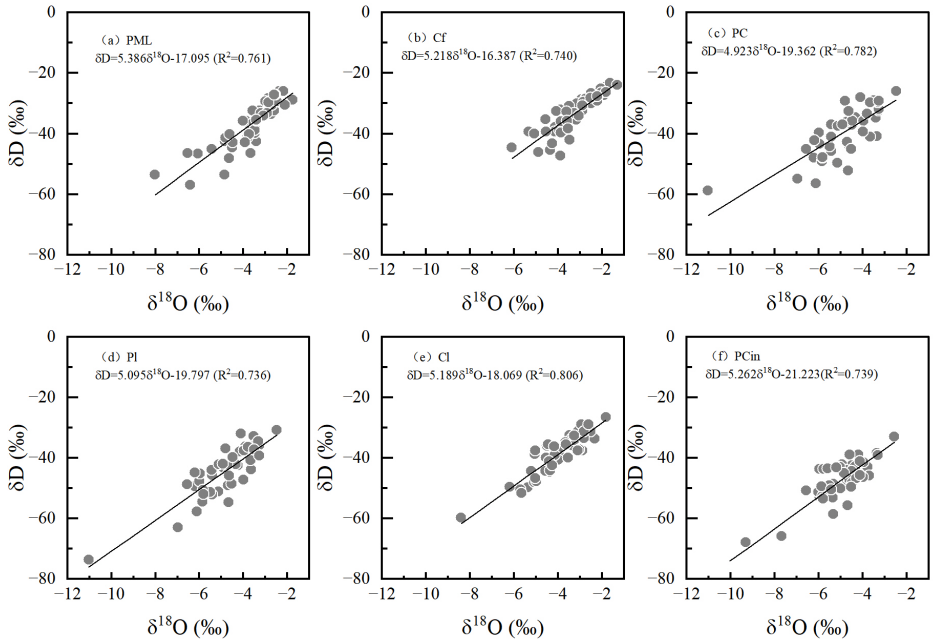

Figure 12. Soil waterline equations for the different woodlands. SWL is the soil waterline equation.

4. Discussion

4.1. The Basic Physical Properties of Soil

In this study, CP and NY existed simultaneously. However, the percentage of NY soil accounted for approximately 30%–45%. This result indicated that the soil permeability of the woodlands in this area was relatively good. CP and NY reflect the ability of forest vegetation to absorb and retain water, respectively. The comparison of the characteristics of soil porosity changes in the six woodlands indicated that the amount of CP was much higher than NY because of the increased vegetation in the woodland. PCin had the maximum CP, which was related to the largest canopy cover in the woodland.

The following characteristics can be obtained by studying soil porosity variation in different soil layers. Compared with deep soils, the topsoil (0–20 cm) had a high TP and NY, which accounted for a large proportion. Therefore, topsoil is the active layer with alternating soil moisture, which is in direct contact with air and is greatly affected by human activities. The TP increased slightly in the 20–30 cm soil layer because the plant roots developed in an umbrella shape in this soil layer. Plant roots enhance pore connectivity [44]. The soil porosity increases because of the large number of roots in the soil. Therefore, the TP increased with soil depth in an N-shaped distribution. These results are inconsistent with the conclusions of some previous studies [45].

The soil water-holding capacity is influenced by soil porosity, soil density, soil particle size, and vegetation growth conditions. Moreover, soil porosity is the most critical parameter of soil water-holding capacity. In this study, the topsoil of each woodland is most affected by human activities. The strong water-holding capacity of the topsoil is due to its loose soil and large TP. Unlike the change in NY, the minimum soil water-holding capacity of the Pl woodland was greater than the Cl woodland. The differences in TP and NY between the Pl and Cl woodlands were 0.01025 and 0.02675, respectively. In particular, the Pl woodland not only had high CP and low NY but also had high soil organic content. This phenomenon resulted in the high permeability, aeration, and water-holding capacity of Pl. Overall, soil MIC is used as a representative factor of soil water-holding capacity. Moreover, the TP has a significant influence on soil water-holding capacity.

4.2. Soil Hydrological Characteristics

Soil-saturated hydraulic conductivity is an important parameter that reflects the characteristics of different woodland TP and water-holding capacity values [46]. In this study, the correlation analysis results showed that soil-saturated hydraulic conductivity decreased with the increase in soil fine particle content. Previous studies showed that as the fine particle content increases from 12% to 50%, the soil hydraulic conductivity decreases by more than 20-fold [47]. The soil texture is detailed when the soil clay content is high. However, the soil-saturated hydraulic conductivity is low when the soil is in a saturated state with a low infiltration water volume.

The PCin woodland had lower soil fine particle content and larger capillary porosity than other woodlands. In addition, soil water infiltration and saturated hydraulic conductivity of the PCin woodland were higher than the other woodlands when the soil moisture reached saturation. Moreover, the soil fine particle content of the Cf woodland was higher than the other woodlands. The Cf woodland had the lowest canopy cover and the smallest TP. In addition, the soil-saturated hydraulic conductivity of the Cf woodland was the smallest of the woodlands. These results are inconsistent with the conclusions of some previous studies [46]. The reason is that the research object is a woodland, and the root system of plants has a significant impact on the soil-saturated hydraulic conductivity. The PCin woodland had the maximum canopy cover, followed by Pl, Cl, PC, PML, and Cf. This finding is consistent with the findings on soil-saturated hydraulic conductivity. However, the soil fine particle content is not completely consistent with soil-saturated hydraulic conductivity. These results indicated that soil-saturated hydraulic conductivity was significantly influenced by canopy cover in this study; this finding is consistent with previous research [21,32].

The trend of soil-saturated hydraulic conductivity with soil depth can be explained by the influence of plants on soil moisture movement. A significant relationship exists between plant root characteristics and the soil water spatial distribution pattern [48]. Root activity has an important impact on soil development [49]. The root systems of shrubs and herbs are distributed in the shallow soil layer, which has a strong capacity for rainfall interception and water consumption. This scenario results in the subsurface soil layer from low aquifers. Therefore, the saturated hydraulic conductivity of the topsoil is higher than the subsurface soil layer. Underground soil has a low fine particle content, high infiltration water, and low water consumption, leading to a high soil-saturated hydraulic conductivity.

The soil macropore outflow rate showed differences with time. It exhibited a trend of increasing uniformly from 0 s to 55 s, decreasing from 55 s to 100 s, and stabilizing after 100 s. At the early stage of water transport, soil macropores had a facilitating effect on soil hydraulic conductivity. The soil macroporosity number density of PCin, Cl, and Pl were 1.704, 1.471, and 1.313 cm^{-3}, respectively. However, the number density of soil macroporosity in the other three woodlands did not exceed 1 $\cdot cm^{-3}$. A slight difference existed in the number of soil macropores and small pores of less than 1.60 mm in the PCin, Cl, and Pl woodlands. Therefore, the soil macropores were gradually filled with water when the water was transported into the soil in the early stage; this finding is consistent with previous research [50]. The water movement process became complicated because the number of soil macropores was large. Moreover, the soil moisture characteristic curves showed fluctuation. In particular, the PCin woodland had the maximum soil pore density, followed by Cl, Pl, PC, PML, and Cf. These differences probably occurred in the canopy cover. Therefore, the average soil infiltration rate in the Pl woodland was greater than the Cl woodland.

Plant roots can significantly improve soil infiltration [50]. The results of the TP indicated that it was consistent with the characteristics of soil water infiltration. Overall, the TP represented the characteristic parameters of soil porosity. The soil macropore number of the 20–30 cm soil layer was slightly greater than the other soil layers in the PML and Cf woodlands. The 0–10 cm soil layer within the four other mixed woodlands had the greatest macropore number and outflow rate. Therefore, the 0–10 cm soil infiltration rate

was the greatest. However, previous studies revealed that the soil infiltration rate and water storage capacity were significantly high in the 0–20 cm soil layer [51]. This finding is probably due to differences in soil water stratification among different study areas. Overall, the infiltration rate of surface soil was the highest. As shown above, the 10–20 cm soil layer had the lowest macropore number, outflow rate, and soil infiltration rate. Therefore, the soil outflow rate was positively related to the number of soil macropores. The number of soil pores in the 30–40 cm soil layer was greater than the 10–20 cm soil layer. However, the opposite was true for TP. According to the definition of porosity, the 30–40 cm soil layer is compact and can easily reach a stable infiltration state.

4.3. Soil Moisture Content

Rainwater is an important material source of soil moisture. The soil moisture potential gradient increased with rainfall, thereby increasing the soil moisture content. The results indicated that the rate of increase in soil moisture content was positively related to MIC ($p < 0.01$). These results are inconsistent with the conclusions of some previous studies [12]. The soil texture in the Loess Plateau area is loess soil; however, the soil particle composition between soil layers has no significant difference [17,31]. Nevertheless, the Taizishan area has viscous yellow-brown soil, and the soil particle composition between soil layers has significant differences.

Soil moisture content changes because of the combination of soil moisture infiltration and evaporation. Precipitation directly supplies the 'material source' of soil water transport. The ground surface was rapidly moist when precipitation was high. However, the water that accumulated in the topsoil continued to supply soil water infiltration after the rainfall event. Soil moisture infiltrates well into the deep soil layers when precipitation is low [52]. The soil moisture content decreased rapidly because of the soil moisture consumption by evaporation and plant growth. The soil moisture content variations of each soil layer initially increased and then decreased with time after rainfall. The wave peak was generally present on the first day after the rainfall event. As shown above, the topsoil moisture content could peak within 24 h from the start of rainfall timing in this study.

The comparison of the mean soil moisture contents of the six forests indicated that the four mixed forests had high contents. These results are consistent with the conclusions of some previous studies [21,53]. The soils under the canopy of conifers showed the most severe soil water repellency levels. In the upper layers, plant transpiration and soil evaporation can consume 60% of the total precipitation [54]. Therefore, the mixed forests had low canopy closure and large water loss, and the upper soil moisture content was low. The trend of the soil moisture content growth rate was consistent at a high rainfall amount but complex at a low rainfall amount [10]. The reason is that soil moisture simultaneously experiences a mixed effect of infiltration and transport after a rainfall event. Infiltration is the main driving force of soil moisture movement when the rainfall amount is high. Nevertheless, the main driving force, which is mainly affected by soil texture, canopy cover, and other factors, is not obvious when rainfall is low.

The vegetation type of Cf includes simple plants, such as ferns and herbs. These shallow-rooted plants have the characteristics of small root morphology and are divided into the 0–20 cm soil layer. Therefore, the TP of the Cf woodland decreased with soil depth. The results indicated that the TP and soil moisture storage capacity of the 10–20 cm soil layer in the Cf woodland were larger than the other soil layers. The small canopy density of the forest strengthens the peak attenuation of the surface soil moisture [13]. Therefore, the growth rate of the subsurface soil moisture content of the 10–20 cm soil layer in Cf was the largest. The maximum value of the soil moisture content growth rate moved between different soil layers. This finding indicated that the magnitude of the forces acting on soil moisture changes over time.

4.4. Hydrogen and Oxygen Isotope Characteristics in Soil Water

According to statistics, the slope and intercept in the soil waterline equation are smaller than those in the atmospheric waterline in this area. The stable isotopic composition of soil water is more enriched than that of atmospheric precipitation. This finding is consistent with previous research [41]. The isotope enrichment in soil water results from the large amounts of soil water evaporation through the topsoil. On the contrary, woodland evaporation is strong in this area. In typical rainfall processes with a long rainfall duration and high rainfall amounts, the isotopic effect leads to the depletion of isotopic values with rainfall duration; this finding is consistent with previous research [18]. Intense evaporation is required for the relative enrichment of soil water δD in sufficient rainfall amounts. The soil water δD in the topsoil layer (0–20 cm) is close to precipitation.

The soil water evaporation decreases with soil depth [55]. Thus, the topsoil water is subject to strong dynamic fractionation caused by the combination of evaporation and precipitation infiltration. The change in δD in topsoil water is obvious. The analysis of the δD value dispersion degree of different soil layers indicated that a large amount of precipitation increases each soil layer's soil water δD dispersion degree. Surface water movement is a complex process influenced by infiltration and evaporation under large precipitation. 'New water' promotes the downward migration of 'old water'. This process requires a strong evaporation effect, resulting in the relative enrichment of deep soil water δD. Moreover, light mass isotope molecules have preferential evaporation properties during soil moisture evaporation, leading to the enrichment of heavy mass isotopes in topsoil water [56]. These results indicated that the topsoil has the lowest moisture content and most pores, the amount of topsoil aqueous phase (from liquid water to gaseous water) is the highest, and the stable isotope is the most enriched.

Soil water infiltration forms differ under different rainfall amounts [55]. In the present study, soil water δD fluctuated between soil water δD and rainwater δD 3 days after the rain. This finding indicated that the main form of soil water infiltration in Cf, PC and Cl was precipitation combined with the soil's original water content under 49.8 mm of rainfall (Figure 10b,c,e). Compared with that before rainfall, the soil water δD in each soil layer on the 1st day after rainfall in Cf, PC and Cl was shifted to different degrees under 23.5 mm of rainfall (Figure 10h,i,k). The soil water δD in the 20–30 cm soil layer was close to the value of rainwater δD, and the soil water δD in the 30–40 cm soil layer was close to that of soil water δD in the 0–20 cm soil layer before rainfall. These results indicated that precipitation in these three woodlands drove topsoil water downwards under moderate rain. Overall, the changes in soil water δD under the three rainfall events indicated that the soil water infiltration form in PML, Cf and PC was the precipitation mixed with original soil water that diffused downwards. In addition, the soil water infiltration form in Pl, Cl and PCin drove out the original soil water.

As shown above, significant differences were detected in the δD and $\delta^{18}O$ values under different rainfall events in this study. These differences were probably produced by the differences in vegetation factors, such as canopy cover and stand canopy closure [1]. Under heavy rainfall, the soil water δD enrichment at the 30–40 cm soil layer in the PML woodland is consistent with previous research [57]. The slope of the PML woodland was greater than 15°. Thus, the upper part of the water was supplied to the sampling site. These results help in understanding that the stand canopy closure and initial soil moisture content directly affect precipitation and soil water evaporation, respectively.

PCin had the highest average soil moisture content and the lowest coefficient of variation because of the large stand canopy closure. The soil moisture loss rate and evaporation decreased when the solar radiation was reduced. Therefore, the soil water δD of PC in woodland was relatively poor, whereas the slope of the soil waterline was large. Overall, the soil water δD was enriched in needleleaved forests and relatively depleted in mixed conifer broadleaved forests. The PCin mixed conifer broadleaved forests exhibited high canopy cover, well-developed root systems, and large soil porosity of topsoil. As shown above, significant differences were detected in the TP under different soil layers. The

mixed conifer broadleaved forest construction mode improved soil quality and increased the content of fine soil particles and soil adhesion.

4.5. Functional Model

In this study, stepwise regression was used to research the effects of basic forestland conditions, soil hydrological properties, and soil particle composition on soil moisture characteristic parameters. According to the stepwise regression results, *Ks*, δD, and $\delta^{18}O$ can be expressed as a power function relationship of field water-holding capacity, slope, and very coarse sand content. Their calculation formulas are as follows:

$$K_s = 0.609\ \mathrm{FWC}^{-0.429}\mathrm{S}^{-0.049}\mathrm{VC}^{-0.701}, \quad (5)$$

$$\delta D = 3.37\ \mathrm{FWC}^{0.358}\mathrm{S}^{-0.656}\mathrm{VC}^{0.403}, \quad (6)$$

$$\delta^{18}O = 1.84\ \mathrm{FWC}^{0.333}\mathrm{S}^{-0.712}\mathrm{VC}^{0.441}, \quad (7)$$

where FWC, S, and VC are the field water-holding capacity, slope, and extremely coarse sand (1–2 mm) particle content, respectively. According to the regression equation, VC was the main parameter affecting soil-saturated hydraulic conductivity, whereas the slope was the main factor affecting soil water δD and $\delta^{18}O$. These results are consistent with previous studies [52].

5. Conclusions

Based on stable isotope technology, this study quantified soil moisture characteristics in different woodlands in Hubei, China. The results indicated that soil hydrological characteristics were greatly influenced by slope, field water-holding capacity, and extremely coarse sand (1–2 mm) particle content, whereas the saturated hydraulic conductivity of the 0–20 cm topsoil layer was 60.073% higher than the 20–40 cm soil layer. The mean soil moisture content of the four mixed forests was higher than the pure forests. The soil waterline equation in this area was $\delta D = 5.626\delta^{18}O - 16.791$ ($R^2 = 0.798$). Moreover, the slope and intercept in the soil waterline equation were smaller than the atmospheric waterline equation. This finding indicated that the woodland evaporation in this area was strong. Surface water movement is a complex process influenced by infiltration and evaporation under large precipitation. The soil water δD of the soil surface (0–20 cm) was close to precipitation δD and fluctuated with time. This phenomenon was related to the few macropores and small evaporation of deep soil. Nevertheless, the soil water δD and $\delta^{18}O$ values of the 20–40 cm soil layer changed flatly with time. Needleleaved woodlands' evaporation was strong, resulting in soil water δD enrichment. Therefore, mixed conifer broadleaved woodlands' evaporation was weak, resulting in relatively depleted soil water. Soil water δD and $\delta^{18}O$ in the topsoil were relatively enriched. The mixture of rainwater and soil water downward diffusion was dominant in pure forests (PML and Cf), whereas the precipitation replacement of old soil water before the rain was dominant in mixed forests (Pl, Cl, and PCin). VC was the main parameter affecting soil-saturated hydraulic conductivity, and the slope was the main factor affecting soil water δD and $\delta^{18}O$.

Author Contributions: Conceptualisation, F.Z. and Y.L.; methodology, F.Z., Y.L. and J.C.; software, F.Z.; validation, F.Z. and J.C.; formal analysis, F.Z.; investigation, F.Z.; resources, F.Z., Y.L. and J.C.; data curation, F.Z.; writing—original draft preparation, F.Z., J.C. and Y.L.; writing—review and editing, F.Z.; visualization, F.Z.; supervision, J.C.; funding acquisition, J.C. All authors have read and agreed to the published version of the manuscript.

Funding: This work was funded by the National Natural Science Foundation of China (grant number 32071839).

Data Availability Statement: The data are available on request from the corresponding author.

Acknowledgments: We thank the National Natural Science Foundation of China (grant number 32071839).

Conflicts of Interest: The authors declare no conflict of interest.

References

1. Tan, S.Y.; Zhao, H.R.; Yang, W.Q.; Tan, B.; Ni, X.Y.; Yue, K.; Zhang, Y.; Wu, F.Z. The effect of canopy exchange on input of base cations in a subalpine spruce plantation during the growth season. *Sci. Rep.* **2018**, *8*, 9373. [CrossRef]
2. Zhang, M.X.; Chen, S.L.; Jiang, H.; Lin, Y.; Zhang, J.M.; Song, X.Z.; Zhou, G.M. Water-Use Characteristics and Physiological Response of Moso Bamboo to Flash Droughts. *Int. J. Environ. Res. Public Health* **2019**, *16*, 2174. [CrossRef]
3. Li, X.; Niu, J.Z.; Xie, B.Y. The effect of leaf litter cover on surface runoff and soil erosion in Northern China. *PLoS ONE* **2014**, *9*, e107789. [CrossRef] [PubMed]
4. Wang, T.; Xu, Q.; Gao, D.Q.; Zhang, B.B.; Zuo, H.J.; Jiang, J. Effects of thinning and understory removal on the soil water-holding capacity in Pinus massoniana plantations. *Sci. Rep.* **2021**, *11*, 13029. [CrossRef]
5. Li, Y.F.; Liu, Y.; Harris, P.; Sint, H.; Murray, P.J.; Lee, M.; Wu, L.H. Assessment of soil water, carbon and nitrogen cycling in reseeded grassland on the North Wyke Farm Platform using a process-based model. *Sci. Total Environ.* **2017**, *603–604*, 27–37. [CrossRef] [PubMed]
6. Qiu, Y.; Fu, B.; Wang, J.; Chen, L. Soil moisture variation in relation to topography and land use in a hillslope catchment of the Loess Plateau, China. *J. Hydrol.* **2001**, *240*, 243–263. [CrossRef]
7. Guendehou, G.H.S.; Liski, J.; Tuomi, M.; Moudachirou, M.; Sinsin, B.; Mäkipää, R. Test of validity of a dynamic soil carbon model using data from leaf litter decomposition in a West African tropical forest. *Geosci. Model Dev. Discuss.* **2013**, *6*, 3003–3032.
8. Meissner, R.; Rupp, H.; Seeger, J.; Ollesch, G.; Gee, G.W. A comparison of waterflux measurements: Passivewick-samplers versus drainagelysimeters. *Eur. J. Soil Sci.* **2010**, *61*, 609–621. [CrossRef]
9. Liu, B.X.; Jia, X.X.; Shao, M.A.; Jia, Y.H. Assessing soil water recovery after converting planted shrubs and grass to natural grass in the northern Loess Plateau of China. *Agric. Water Manag.* **2022**, *264*, 107490. [CrossRef]
10. Poblador, S.; Thomas, Z.; Rousseau-Gueutin, P.; Sabate, S.; Sabater, F. Riparian forest transpiration under the current and projected Mediterranean climate: Effects on soil water and nitrate uptake. *Ecohydrology* **2019**, *12*, e2043. [CrossRef]
11. Chen, L.D.; Huang, Z.L.; Gong, J.; Fu, B.J.; Huang, Y.L. The effect of land cover/vegetation on soil water dynamic in the hilly area of the Loess Plateau, China. *Catena* **2007**, *70*, 200–208. [CrossRef]
12. Su, B.Q.; Shangguan, Z.P. Decline in soil moisture due to vegetation restoration on the Loess Plateau of China. *Land Degrad. Dev.* **2019**, *30*, 290–299. [CrossRef]
13. O'Donnell, F.C.; Donager, J.; Sankey, T.; Lopez, S.M.; Springer, A.E. Vegetation structure controls on snow and soil moisture in restored ponderosa pine forests. *Hydrol. Process.* **2021**, *35*, e14432. [CrossRef]
14. Moon, H.; Guillod, B.P.; Gudmundsson, L.; Seneviratne, S.I. Soil Moisture Effects on Afternoon Precipitation Occurrence in Current Climate Models. *Geophys. Res. Lett.* **2019**, *46*, 1861–1869. [CrossRef] [PubMed]
15. Yu, B.W.; Liu, G.H.; Liu, Q.S. Effects of land use changes for ecological restoration on soil moisture on the Chinese Loess Plateau: A meta-analytical approach. *J. For. Res.* **2020**, *31*, 443–452. [CrossRef]
16. Gu, X.; Zhang, Q.; Li, J.; Singh, V.; Liu, J.; Sun, P.; Cheng, C. Attribution of Global Soil Moisture Drying to Human Activities: A Quantitative Viewpoint. *Geophys. Res. Lett.* **2019**, *46*, 2573–2582. [CrossRef]
17. Mei, X.M.; Ma, L.; Zhu, Q.K.; Wang, S.; Zhang, D.; Wang, Y. Responses of soil moisture to vegetation restoration type and slope length on the loess hillslope. *J. Mt. Sci.* **2018**, *15*, 548–562. [CrossRef]
18. Snelgrove, J.R.; Buttle, J.M.; Tetzlaff, D. Importance of rainfall partitioning in a northern mixed forest canopy for soil water isotopic signatures in ecohydrological studies. *Hydrol. Process.* **2020**, *34*, 284–302. [CrossRef]
19. Hayati, E.; Abdi, E.; Saravi, M.M.; Nieber, J.L.; Majnounian, B.; Chirico, G.B.; Wilson, B.; Nazarirad, M. Soil water dynamics under different forest vegetation cover: Implications for hillslope stability. *Earth Surf. Process. Landforms* **2018**, *43*, 2106–2120. [CrossRef]
20. Rog, I.; Tague, C.; Jakoby, G.; Megidish, S.; Yaakobi, A.; Wagner, Y.; Klein, T. Interspecific Soil Water Partitioning as a Driver of Increased Productivity in a Diverse Mixed Mediterranean Forest. *J. Geophys. Res. Biogeosci.* **2021**, *126*, e2021JG006382. [CrossRef]
21. Wei, L.; Qiu, Z.; Zhou, G.; Zuecco, G.; Liu, Y.; Wen, Y. Soil water hydraulic redistribution in a subtropical monsoon evergreen forest. *Sci. Total Environ.* **2022**, *835*, 155437. [CrossRef] [PubMed]
22. Poca, M.; Cingolani, A.M.; Gurvich, D.E.; Whitworth-Hulse, J.I.; Saur Palmieri, V. The degradation of highland woodlands of central Argentina reduces their soil water storage capacity. *Ecol. Austral* **2018**, *28*, 235–248.
23. Archer, N.A.L.; Bonell, M.; Coles, N.; MacDonald, A.M.; Auton, C.A.; Stevenson, R. Soilcharacteristics and land cover relationships on soil hydraulic conductivity at a hillslopes cale: A view towards local flood management. *J. Hydrol.* **2013**, *497*, 208–222. [CrossRef]
24. Nie, C.; Huang, Y.F.; Zhang, S.; Yang, Y.T.; Zhou, S.; Lin, C.J.; Wang, G.Q. Effects of soil water content on forest ecosystem water use efficiency through changes in transpiration/evapotranspiration ratio. *Agric. For. Meteorol.* **2021**, *308–309*, 108605. [CrossRef]
25. Wu, W.J.; Li, H.J.; Feng, H.; Si, B.C.; Chen, G.J.; Meng, T.F.; Li, Y.; Siddique, K. Precipitation dominates the transpiration of both the economic forest (*Malus pumila*) and ecological forest (*Robinia pseudoacacia*) on the Loess Plateau after about 15 years of water depletion in deep soil. *Agric. For. Meteorol.* **2021**, *297*, 108244. [CrossRef]

26. Chen, L.L.; Mu, X.M.; Yuan, Z.Y.; Deng, Q.; Chen, Y.L.; Yuan, L.Y.; Ryan, L.T.; Kallenbach, R.L. Soil nutrients and water affect the age-related fine root biomass but not production in two plantation forests on the Loess Plateau, China. *J. Arid. Environ.* **2016**, *135*, 173–180. [CrossRef]
27. Jiao, L.; Lu, N.; Fang, W.W.; Li, Z.S.; Wang, J.; Jin, Z. Determining the independent impact of soil water on forest transpiration: A case study of a black locust plantation in the Loess Plateau, China. *J. Hydrol.* **2019**, *572*, 671–681. [CrossRef]
28. Ilek, A.; Kucza, J.; Szostek, M. The effect of the bulk density and the decomposition index of organic matter on the water storage capacity of the surface layers of forest soils. *Geoderma* **2017**, *285*, 27–34. [CrossRef]
29. Zhu, X.; He, Z.B.; Du, J.; Chen, L.F.; Lin, P.F.; Li, J. Temporal variability in soil moisture after thinning in semi-arid Picea crassifolia plantations in northwestern China. *For. Ecol. Manag.* **2017**, *401*, 273–285. [CrossRef]
30. Tian, J.; Zhang, B.; He, C.; Yang, L. Variability in Soil Hydraulic Conductivity and Soil Hydrological Response Under Different Land Covers in the Mountainous Area of the Heihe River Watershed, Northwest China. *Land Degrad. Dev.* **2017**, *28*, 1437–1449. [CrossRef]
31. Fang, X.N.; Zhao, W.W.; Wang, L.X.; Feng, Q.; Zhang, X. Spatial variations of deep soil moisture and the influencing factors in the Loess Plateau, China. *Hydrol. Earth Syst. Sci. Discuss.* **2016**, *2016*, 1–42.
32. Gou, Q.; Zhu, Q. Response of deep soil moisture to different vegetation types in the Loess Plateau of northern Shannxi, China. *Sci. Rep.* **2021**, *11*, 15098. [CrossRef]
33. Penna, D.; Hopp, L.; Scandellari, F.; Allen, S.T.; Benettin, P.; Beyer, M.; Geris, J.; Klaus, J.; Marshall, J.D.; Schwendenmann, L.; et al. Ideas and perspectives: Tracing terre striale cosystem water fluxesusing hydrogen and oxygen stable isotopes-challenges and opportunities from aninter disciplinary perspective. *Biogeosciences* **2018**, *15*, 6399–6415. [CrossRef]
34. Oerter, E.J.; Bowen, G. In situ monitoring of H and O stable isotopes in soil water reveals ecohydrologic dynamics in managed soil systems. *Ecohydrology* **2017**, *10*, e1841. [CrossRef]
35. Zheng, L.J.; Ma, J.J.; Sun, X.H.; Guo, X.H.; Cheng, Q.Y.; Shi, X.K. Estimating the Root Water Uptake of Surface-Irrigated Apples Using Water Stable Isotopes and the Hydrus-1D Model. *Water* **2018**, *10*, 1624. [CrossRef]
36. Liu, T.Y.; Chen, M.X.; Zhang, Y.J.; Zhu, F.Y.; Liu, Y.G.; Tian, Y.; Fernie, A.R.; Ye, N.H.; Zhang, J.H. Comparative metabolite profiling of two switch grass eco-types reveals differences in droughts tress responses and rhizosheath weight. *Planta* **2019**, *250*, 1355–1369. [CrossRef] [PubMed]
37. Wang, J.; Fu, B.J.; Lu, N.; Zhang, L. Seasonal change in root liquids uptake patterns of photosynthetic eukaryotes species in the sem-arid Loes Plateau. *Sci Env.* **2018**, *609*, 27–37.
38. Goldsmith, G.R.; Allen, S.T.; Braun, S.; Engbersen, N.; Gonzalez-Quijano, C.R.; Kirchner, J.W.; Siegwolf, R. Spatial variation in throughfall, soil, and plant water isotopes in a temperate forest. *Ecohydrology* **2019**, *12*, e2059. [CrossRef]
39. Zhou, J.; Fu, B.J.; Gao, G.Y.; Lu, Y.H.; Wang, S. Anintegrated probabilistic assessment to analyses to chasticity of soil erosion in differentres toration vegetation types. *Hydrol. Earth Syst. Sci.* **2017**, *21*, 1491–1514. [CrossRef]
40. Jia, G.D.; Yu, X.X.; Deng, W.P. Seasonal water use patterns of semi-arid plants in China. *For. Chron.* **2013**, *89*, 169–177. [CrossRef]
41. Li, Y.C.; Zhu, F.F.; Wang, Y.; Cheng, J.H. Soil Water Use Strategies of Dominant Tree Species Basedon Stable Isotopes in Subtropical Regions, Central China. *Water* **2022**, *14*, 954. [CrossRef]
42. Zhang, J.; Lei, T.; Yin, Z.; Hu, Y.; Yan, X. Effects of times teplength and positioning location on ring-measured infiltration rate. *Catena* **2017**, *157*, 344–356. [CrossRef]
43. Jian, W.; Fu, B.; Nan, L.; Li, Z. Variation in water of plants based on isotopes in the semi-arid Loess Plateau. *Sci. Total Environ.* **2017**, *612*, 42–53.
44. Whalley, W.R.; Riseley, B.; Leeds-Harrison, P.B.; Bird, N.; Leech, P.K.; Adderley, W.P. Structuraldifferencesbetweenbulk and rhizospheresoil. *Eur. J. Soil Sci.* **2005**, *56*, 353–360. [CrossRef]
45. Bodner, G.; Leitner, D.; Kaul, H.P. Coarse and fine root plants affect pore size distributions differently. *Plant Soil* **2014**, *380*, 133–151. [CrossRef] [PubMed]
46. Ilek, A.; Kucza, J.; Witek, W. Using undisturbed soils amples to study how rock fragments and soil macropores affect the hydraulic conductivity of forest stony soils: Some methodological aspects. *J. Hydrol.* **2019**, *570*, 132–140. [CrossRef]
47. Fan, J.; Rowe, R.K.; Brachman, R.W. Compressibility and perme ability of sand-silttailings mixtures. *Can. Geotech. J.* **2022**, *59*, 1348–1357. [CrossRef]
48. Kizito, F.; Dragila, M.; Sene, M.; Lufafa, A.; Diedhiou, I.; Dick, R.P.; Selker, J.S.; Dossa, E.; Khouma, M.; Badiane, A. Seasonal soil water variation and root patterns between two semi-arid shrubs co-existing with Pearl millet in Senegal, West Africa. *J. Arid. Environ.* **2006**, *67*, 436–455. [CrossRef]
49. Soleimani, R.; Hosseini, A. The impact of Persianoak (QuercusbrantiiLindl.) on soil characteristics in a declining forest. *J. For. Res.* **2020**, *31*, 2359–2366. [CrossRef]
50. Hao, H.X.; Wei, Y.J.; Cao, D.N.; Guo, Z.L.; Shi, Z.H. Vegetation restoration and fine roots promote soil infiltrability in heavy-textured soils. *Soil Tillage Res.* **2020**, *198*, 104542. [CrossRef]
51. Chen, L.; Yuan, Z.; Shao, H.; Wang, D.; Mu, X. Effects of Thinning Intensities on Soil Infiltration and Water Storage Capacityina Chinese Pine-Oak Mixed Forest. *Sci. World J.* **2014**, *2014*, 268157.
52. Huang, J.; Wu, P.T.; Zhao, X.N. Effects of rainfall intensity, underlying surface and slope gradient on soil infiltration under simulated rainfall experiments. *Catena* **2013**, *104*, 93–102. [CrossRef]

53. Alanis, N.; Hernandez-Madrigal, V.M.; Cerda, A.; Munoz-Rojas, M.; Zavala, L.M.; Jordan, A. Spatial Gradients of Intensity and Persistence of Soil Water Repellency Under Different Forest Types in Central Mexico. *Land Degrad. Dev.* **2017**, *28*, 317–327. [CrossRef]
54. Oki, T.; Kanae, S. Global hydrological cycles and world water resources. *Science* **2006**, *313*, 1068–1072. [CrossRef]
55. Che, C.; Zhang, M.; Argiriou, A.A.; Wang, S.; Yung, P. The stable isotopic composition of different water bodies at the soil-plant-atmosphere continuum (SPAC) of the western Loess Plateau, China. *Water* **2019**, *11*, 1742. [CrossRef]
56. Matthias, S.; Doerthe, T.; Chris, S. Soil water stable isotopes reveal evaporation dynamics at the soil–plant–atmosphere interface of the critical zone. *Hydrol. Earth Syst. Sci.* **2017**, *21*, 3839–3858.
57. Han, J.; Duan, X.; Zhao, Y.; Li, M. Characteristics of Stable Hydrogen and Oxygen Isotopes of Soil Moisture under Different Land Use in Dry Hot Valley of Yuanmou. *Open Chem.* **2019**, *17*, 105–115. [CrossRef]

Disclaimer/Publisher's Note: The statements, opinions and data contained in all publications are solely those of the individual author(s) and contributor(s) and not of MDPI and/or the editor(s). MDPI and/or the editor(s) disclaim responsibility for any injury to people or property resulting from any ideas, methods, instructions or products referred to in the content.